



## Shape-Independent Limits to Near-Field Radiative Heat Transfer

Owen D. Miller,<sup>1</sup> Steven G. Johnson,<sup>1</sup> and Alejandro W. Rodriguez<sup>2</sup>

<sup>1</sup>*Department of Mathematics, Massachusetts Institute of Technology, Cambridge, Massachusetts 02139, USA*

<sup>2</sup>*Department of Electrical Engineering, Princeton University, Princeton, New Jersey 08544, USA*

(Received 6 April 2015; published 12 November 2015)

We derive shape-independent limits to the spectral radiative heat transfer rate between two closely spaced bodies, generalizing the concept of a blackbody to the case of near-field energy transfer. Through conservation of energy and reciprocity, we show that each body of susceptibility  $\chi$  can emit and absorb radiation at enhanced rates bounded by  $|\chi|^2/\text{Im}\chi$ , optimally mediated by near-field photon transfer proportional to  $1/d^2$  across a separation distance  $d$ . Dipole-dipole and dipole-plate structures approach restricted versions of the limit, but common large-area structures do not exhibit the material enhancement factor and thus fall short of the general limit. By contrast, we find that particle arrays interacting in an idealized Born approximation (i.e., neglecting multiple scattering) exhibit both enhancement factors, suggesting the possibility of orders-of-magnitude improvement beyond previous designs and the potential for radiative heat transfer to be comparable to conductive heat transfer through air at room temperature, and significantly greater at higher temperatures.

DOI: 10.1103/PhysRevLett.115.204302

PACS numbers: 44.40.+a, 41.20.Jb

Heat exchange mediated by photons, or radiative heat transfer, can be dramatically modified for bodies separated by small gaps [1–7]. We exploit energy-conservation and reciprocity principles to derive fundamental limits to the near-field spectral heat flux between closely spaced bodies of arbitrary shape, given only their material susceptibilities  $\chi(\omega)$  and their separation distance  $d$ . Our approach enables us to define optimal absorbers and emitters in the near field, which contrast sharply with far-field blackbodies: their response is bounded by the amplitude of their volume polarization currents, rather than their surface absorptivities, and maximum energy transfer requires coordinated design of the two bodies (whereas the far-field limit derives from the properties of a single blackbody). These distinguishing characteristics lead to two possible enhancements relative to blackbody emission: a material enhancement factor  $|\chi(\omega)|^2/\text{Im}\chi(\omega)$  that represents the maximum absorber and emitter polarization currents, and a near-field enhancement factor  $1/d^2$  that represents maximum interaction between currents in free space. We show that restricted versions of our limits can be approached for sphere-sphere and sphere-plate configurations. For two extended structures, however, common planar geometries—including bulk metals [8–17], metamaterials [18–24], and thin films [25–31]—exhibit flux rates orders of magnitude short of the limits because they do not satisfy the optimal-absorber condition. Instead, we find that idealized plasmonic-particle arrays, interacting within a Born approximation with negligible multiple scattering, approach the limits at selected frequencies, and that the possibility of reaching the limits, even over a narrow bandwidth (a desirable feature for thermophotovoltaics [7,32–35]), would represent an orders-of-magnitude improvement over current designs.

A ray-optical blackbody absorbs every photon incident upon its surface, which by reciprocity (Kirchhoff's law) yields its emissivity and the blackbody limit to thermal radiation [36]. At wavelength and subwavelength scales, nanostructures can exhibit optical cross sections much larger than their physical cross sections [37], making it difficult even to define quantities like emissivity. A further difficulty in the near field is the presence of evanescent waves, which can increase transmitted power but only through interference with reflected waves [38]. Although the possibility of enhancement beyond the blackbody limit was realized by Rytov, Polder, and others in the 1950s [1,2], efforts to find underlying limits have been restricted to planar structures with translation symmetry (including metamaterials), without consideration of material loss [10,15–17,21,30]. Spherical-harmonic [39,40] and Green's-function [41] limits are difficult to apply in the near field where a large but unknown number of spherical harmonics can be excited by general shapes [42].

Without reference to particular structures or symmetries, assuming only linear electromagnetism, we translate the reciprocity principle to the near field by applying it to polarization currents within the bodies. Dipoles in vacuum exchange energy at a rate limited by the energy density of an outgoing free-space wave [43]. As we show below, the maximum energy transfer between material bodies occurs when the currents within the bodies couple individually at the dipole-dipole limit, amplified by material enhancement factors. These conditions allow for much greater heat transfer than has previously been shown possible.

Radiative heat exchange is depicted schematically in Fig. 1(a): fluctuating currents arise in body 1 at temperature  $T_1$ , and transfer energy to body 2 at a rate of [4]

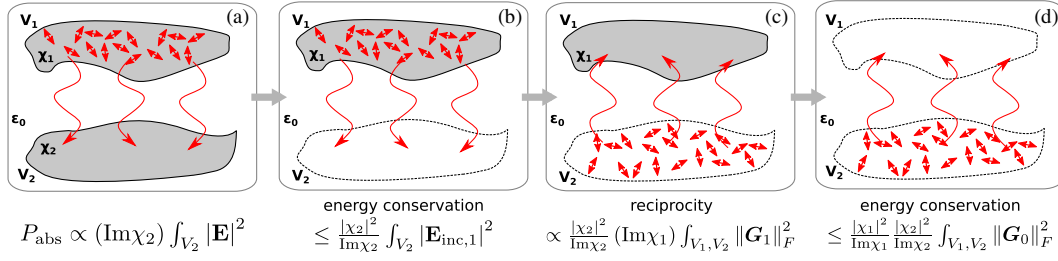


FIG. 1 (color online). (a) Radiative heat transfer: Fluctuating currents in an emitter (body 1, susceptibility  $\chi_1$ ) generate a field  $\mathbf{E}_{\text{inc},1}$  and transfer energy to an absorber (body 2, susceptibility  $\chi_2$ ) at a rate  $P_{\text{abs},2}$ . (b) Energy conservation bounds  $P_{\text{abs},2}$  in terms of  $\mathbf{E}_{\text{inc},1}$ , and a resonant enhancement factor  $|\chi_2|^2/\text{Im}\chi_2$ . (c) The sources and “receivers” can be exchanged by reciprocity, whereupon (d) absorption in body 1 is bounded, yielding a spectral-flux limit determined by  $\chi_1, \chi_2$ , and the free-space GF  $\mathbf{G}_0$ . For near-field transfer the GF integral is  $\sim 1/d^2$ , for separation  $d$ .

$$H_{1 \rightarrow 2} = \int_0^\infty \Phi(\omega) [\Theta(\omega, T_1) - \Theta(\omega, T_2)] d\omega, \quad (1)$$

where  $\Phi(\omega)$  is a temperature-independent energy flux and  $\Theta$  is the Planck spectrum.  $\Phi(\omega)$  is the designable quantity of interest, to be tailored as a function of frequency depending on the application and available materials.

*Limits.*—The spectral heat flux  $\Phi(\omega)$  is the power absorbed in body 2 from fluctuating sources in body 1 (or vice versa). In recent work [42] we have bounded the scattering properties of any dissipative medium excited by a known, externally generated incident field. The bounds arise from the functional dependencies of power expressions with respect to induced currents: absorption is a quadratic functional, whereas extinction (absorption + scattering), given by the optical theorem [44–47], is only a linear functional. Energy conservation requires that extinction be greater than absorption, which imposes a bound on the magnitude of the excited currents. Radiative heat transfer, however, involves sources *within* one of the scatterers, preventing a simple optical theorem.

To circumvent this issue we reframe the scattering problem (without approximation). We define the “incident” field to be the unknown field emanating from body 1, and the “scattered” field to arise only with the introduction of body 2. For a Green’s function (GF)  $\mathbf{G}^1$  that is the field of dipole in the presence of body 1, the fields are given by a standard integral-equation separation [48],  $\mathbf{E}_{\text{inc},1} = (i/\epsilon_0\omega) \int_{V_1} \mathbf{G}_1 \mathbf{J}$  and  $\mathbf{E}_{\text{scat},1} = \int_{V_2} \mathbf{G}_1 \mathbf{P}$ , where  $\mathbf{J}$  are the stochastic source currents in body 1,  $\mathbf{P}$  is the polarization field induced in body 2, and  $\epsilon_0$  is the vacuum permittivity. This decomposition permits an optimal theorem with respect to body 2, such that its extinction is proportional to  $\text{Im} \int_{V_2} \overline{\mathbf{E}_{\text{inc},1}} \cdot \mathbf{P}$  (its absorption [44] is proportional to  $\int_{V_2} |\mathbf{P}|^2$ ). The energy-conservation arguments from above imply that absorption in body 2 is bounded,

$$P_{\text{abs},2} \leq \frac{\epsilon_0\omega}{2} \frac{|\chi_2(\omega)|^2}{\text{Im}\chi_2(\omega)} \int_{V_2} |\mathbf{E}_{\text{inc},1}(\mathbf{x}_2)|^2, \quad (2)$$

which is formally derived by variational calculus [42]. To achieve this limit, the optimal polarization field must be proportional to the incident field,  $\mathbf{P} \sim \mathbf{E}_{\text{inc},1}$ , to maximize

the extinction overlap integral. In the near field, where source fields rapidly decay, negative-permittivity metals that support surface-plasmon modes can achieve this condition, as we will demonstrate.

The limit in Eq. (2) reduces the optimal-flux problem to a question of how large the emitted field  $\mathbf{E}_{\text{inc},1}$  can be in  $V_2$ . Inserting  $\mathbf{E}_{\text{inc},1}$  into Eq. (2) yields an integral of the stochastic currents, which is determined by the fluctuation-dissipation theorem [4],  $\langle J_j(\mathbf{x}, \omega), J_k(\mathbf{x}', \omega) \rangle = 4\epsilon_0\omega\Theta(\omega, T_1) \text{Im}[\chi(\omega)] \delta_{jk} \delta(\mathbf{x} - \mathbf{x}')/\pi$ , such that the ensemble-averaged emitted field at  $\mathbf{x}_2$  in  $V_2$  is  $\langle |\mathbf{E}_{\text{inc},1}(\mathbf{x}_2)|^2 \rangle = 4\epsilon_0\omega\Theta(\text{Im}\chi_1) \int_{V_1} \|\mathbf{G}_1(\mathbf{x}_2, \mathbf{x}_1)\|_F^2$ , where  $\|\cdot\|_F$  denotes the Frobenius norm [49]. By reciprocity [50] one can exchange the positions in the integrand,  $\mathbf{x}_1 \leftrightarrow \mathbf{x}_2$  (while transposing the GF, but the transpose does not affect the norm), such that emission from  $V_1$  is equivalent to *absorption* for free-space sources in  $V_2$ , as in Fig. 1(c). Absorption is bounded by energy conservation [42], limiting the emitted-field magnitude

$$\langle |\mathbf{E}_{\text{inc},1}(\mathbf{x}_2)|^2 \rangle \leq 4\epsilon_0\omega\Theta \frac{|\chi_1|^2}{\text{Im}\chi_1} \int_{V_1} \|\mathbf{G}_0(\mathbf{x}_1, \mathbf{x}_2)\|_F^2, \quad (3)$$

where  $\mathbf{G}_0$  is the *free-space* GF, cf. Fig. 1(d). Inserting Eq. (3) into Eq. (2) and separating the Planck spectrum by Eq. (1), the maximum flux between two bodies is

$$\Phi(\omega) \leq \frac{2}{\pi} \frac{|\chi_1(\omega)|^2 |\chi_2(\omega)|^2}{\text{Im}\chi_1(\omega) \text{Im}\chi_2(\omega)} \int_{V_1} \int_{V_2} \|\mathbf{G}_0(\mathbf{x}_1, \mathbf{x}_2)\|_F^2. \quad (4)$$

The limit of Eq. (4) can be further simplified. In the near field,  $\mathbf{G}_0$  is ideally dominated by the quasistatic term  $\sim 1/r^3$ , which is primarily responsible for the evanescent waves that enable greater-than-blackbody heat-transfer rates [4,7]. Dropping higher-order terms (further discussed in Ref. [51]), we bound Eq. (4) by integrating over the infinite half-spaces containing  $V_1$  and  $V_2$ , assuming a separating plane between the two bodies. (If not, e.g., between two curved surfaces, only the coefficients change.) For bodies separated by a distance  $d$ , the integral over the (infinite) area  $A$  is given by Ref. [51]  $\int_{V_1, V_2} \|\mathbf{G}_0\|_F^2 = A/32\pi d^2$ , yielding flux limits per area or relative to a blackbody with flux  $\Phi_{\text{BB}} = k^2 A/4\pi^2$  [4]:

$$\frac{\Phi(\omega)}{A} \leq \frac{1}{16\pi^2 d^2} \frac{|\chi_1(\omega)|^2 |\chi_2(\omega)|^2}{\text{Im}\chi_1(\omega) \text{Im}\chi_2(\omega)}, \quad (5)$$

$$\frac{\Phi(\omega)}{\Phi_{\text{BB}}(\omega)} \leq \frac{1}{4(kd)^2} \frac{|\chi_1(\omega)|^2 |\chi_2(\omega)|^2}{\text{Im}\chi_1(\omega) \text{Im}\chi_2(\omega)}. \quad (6)$$

Equations (4)–(6) are fundamental limits to the near-field spectral heat flux between two bodies and form the central results of this Letter. They arise from basic limitations to the currents that can be excited in dissipative media, and their derivations further suggest physical characteristics of the optimal response in near-field heat transfer: an optimal emitter enhances and absorbs near-field waves from reciprocal external sources in the absence of the absorber, whereas an optimal absorber enhances and absorbs near-field waves from the emitter in the presence of the emitter. These principles can be understood by working backwards through Fig. 1. The optimal-emitter condition identifies the largest field that can be generated in an exterior volume ( $V_2$ ) by considering the reciprocal absorption problem, per Fig. 1(c). Reinserting the absorber, cf. Fig. 1(b), should not reflect the emitted field but rather enhance and absorb it. Because heat flux is symmetric with respect to absorber-emitter exchange, both bodies should satisfy each condition (induced currents proportional to source fields). Equation (4) can be interpreted as sources throughout the emitter generating free-space dipolar fields  $\mathbf{G}^0$  enhanced by  $|\chi_1|^2/\text{Im}\chi_1$ , which are further enhanced by  $|\chi_2|^2/\text{Im}\chi_2$  and absorbed. The dipole-dipole interactions are bounded by their separation distance [43,54], leading to simple shape-independent limits in Eqs. (4)–(6). Ideal structures that achieve these limits can have significantly greater heat transfer than blackbodies, even if their spectral flux has a narrow bandwidth. Whereas the heat transfer between blackbodies in the far field is  $H/A = \sigma_{\text{SB}} T^4$ , where  $\sigma_{\text{SB}}$  is the Stefan-Boltzmann constant [36], a straightforward calculation [51] shows that ideal near-field heat exchange over a narrow bandwidth  $\Delta\omega/\omega = \text{Im}\chi/|\chi|$ , typical of plasmonic systems [55,56], can achieve per-area transfer rates of

$$\frac{H}{A} \approx \sigma_{\text{SB}} T^4 \frac{2}{7(kd)^2} \frac{|\chi|^3}{\text{Im}\chi}, \quad (7)$$

exhibiting both distance and material enhancements relative to the Stefan-Boltzmann rate.

The limits generalize [51] to local media with tensor susceptibilities via the replacement  $|\chi|^2/\text{Im}\chi \rightarrow \|\chi(\text{Im}\chi)^{-1}\chi^\dagger\|_2$ . Nonlocal effects, which appear below 10 nm length scales [57], and which regularize the  $1/d^2$  divergence [4], are outside the scope of these limits, but we believe that a generalization to nonlocal  $\chi$  is possible and have preliminary results [58] suggesting that “hydrodynamic” [59,60] nonlocal materials cannot surpass the local- $\chi$  bounds.

*Dipolar interactions.*—If one of the bodies is small enough for its response to be dipolar, the optimal-absorber

and optimal-emitter conditions converge: the polarization currents induced in each structure by free-space dipoles in place of the opposite structure must be proportional to the incident fields. This condition is satisfied for two-dipole transfer, and the enhancement of the emitted and absorbed fields is possible via “plasmonic” resonances in metallic nanoparticles. For two identical particles with volumes  $V$ , tip-to-center-of-mass distances  $r$ , and tip-to-tip separation  $d$ , Eq. (4) limits the flux

$$[\Phi(\omega)]_{\text{dipole-dipole}} \leq \frac{3}{4\pi^3} \frac{|\chi_1(\omega)|^2 |\chi_2(\omega)|^2}{\text{Im}\chi_1(\omega) \text{Im}\chi_2(\omega)} \frac{V^2}{(2r+d)^6}. \quad (8)$$

The radiative flux [4] between quasistatic metal spheres peaks at the limit given by Eq. (8).

Heat transfer between a dipole and an extended structure is limited by integrating over the half-space occupied by any extended structure, yielding a maximum flux

$$[\Phi(\omega)]_{\text{dipole-to-ext}} \leq \frac{1}{8\pi^2} \frac{|\chi_1(\omega)|^2 |\chi_2(\omega)|^2}{\text{Im}\chi_1(\omega) \text{Im}\chi_2(\omega)} \frac{V}{(r+d)^3}, \quad (9)$$

where  $r+d$  is the distance between the extended structure and the particle’s center. Heat flux between a sphere and a bulk metal, each supporting a plasmonic mode, can achieve half of the maximum flux [4,51,61] if the resonances align. This geometry falls short by a factor of 2 because planar surface plasmons exist only for TM polarization [62], and thus the planar structure reflects near-field TE-polarized light emitted by the sphere. Neither structure exhibits the  $1/d^2$  enhancement factor, which for dipolar coupling ( $\sim 1/d^6$ ) requires interactions over two extended areas.

Figure 2 compares flux rates for sphere-sphere (orange circles) and sphere-plate (blue circles) geometries, computed by the fluctuating-surface current method [63–65], to the limits of Eqs. (8) and (9) (orange and blue dashed lines). The spheres are modeled by Drude susceptibilities [44] with plasma frequency  $\omega_p$  and loss rate  $\gamma = 0.1\omega_p$ . The “plate” is simulated by a very large ellipsoid (volume  $\approx 7000\times$  larger than the sphere) comprising a material with a modified plasma frequency,  $\omega_{p,\text{pl}} = \sqrt{2/3}\omega_p$ , and a modified loss rate,  $\gamma_{\text{pl}} = 2\gamma/3$ , to align the resonant frequencies of the sphere and plate without modifying the flux limit. In each case the separation distance  $d = 0.1c/\omega_{\text{res}}$  and the sphere radii are  $r = d/5$ . The computations support the analytical result that the dipolar limits can be approached to within at least a factor of 2.

*Extended structures.*—For extended structures that do not behave like single dipoles, the optimal-absorber constraint is more demanding in that the absorber should enhance the emitted field while accounting for interactions between the two bodies. We will show that common planar structures do not exhibit this behavior but that nanostructured media offer the possibility of approaching it.

Bulk metals (negative-permittivity materials) support surface plasmons that enable greater-than-blackbody heat

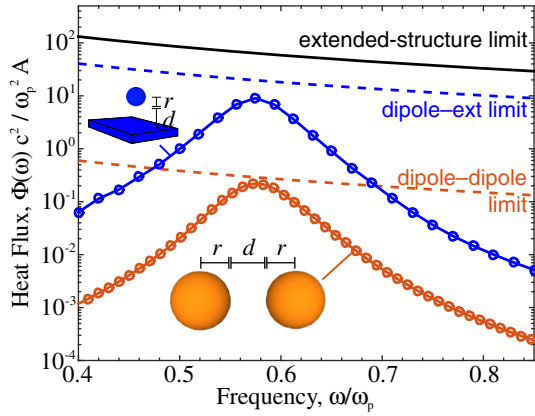


FIG. 2 (color online). Comparison of heat flux in sphere-sphere and sphere-plate structures to the analytical limits of Eqs. (8) and (9). Two Drude metal spheres (orange circles, fit to a solid line) approach the dipole-dipole limit (dashed orange line) at their resonant frequency,  $\omega_{\text{res}} \approx \omega_p / \sqrt{3}$ . A sphere and a plate (blue circles) approach within a factor of 2 of the limit between dipolar and extended objects (dashed blue line), if the material resonance of the plate is slightly modified (see text). In each case the separation is  $d = 0.1c/\omega_{\text{res}}$ , with sphere radii  $r = d/5$ . The flux rates exhibit the material enhancement factor  $|\chi|^4 / (\text{Im}\chi)^2$ , but not the near-field enhancement factor, due to the lack of large-area interactions. The sphere area  $A$  is taken to be the cross-section  $\pi r^2$ .

flux at their resonant frequency. Individually, a single metal interface nearly satisfies the optimal-emitter condition, emitting near-field waves over a broad bandwidth of surface-parallel wave vectors (which enabled the nearly optimal sphere-plate transfer above). However, when a second metal is brought close to the first, it *reflects* most of the incident field, except over a narrow wave vector bandwidth, due to multiple-scattering effects between the

bodies. The failure of the two-metal geometry to achieve the optimal-absorber condition leads to a peak spectral heat flux, at the surface-plasmon frequency  $\omega_{\text{sp}}$ , of approximately [51]

$$\left[ \frac{\Phi(\omega_{\text{sp}})}{A} \right]_{\text{plate-to-plate}} = \frac{1}{4\pi^2 d^2} \ln \left[ \frac{|\chi|^4}{4(\text{Im}\chi)^2} \right], \quad (10)$$

which is significantly smaller than the limit in Eq. (5) due to the weak, logarithmic material enhancement. Equation (10) appears to be new and is a significantly better approximation than planar bounds that do not account for material loss [10,16], as discussed in the Supplemental Material [51]. The shortcomings of the bulk-metal interactions cannot be overcome with simple metamaterial or thin-film geometries. The flux rate between hyperbolic metamaterials (HMMs) is material independent [21,51]. Optimal thin films behave similarly to HMMs [31], thereby also falling short of the limits. “Elliptical” metamaterials, with nearly isotropic effective permittivities, exhibit resonances for  $\chi_{\text{eff}} \approx -2$  and thus transfer heat at a rate similar to Eq. (10), limited by the same interference effects discussed above, and because  $|\chi_{\text{eff}}|^4 \ll |\chi|^4$ .

Figures 3(a) and 3(b) demonstrate the shortcomings of such structures, showing the computed flux between mirror images of thin-film (purple), hyperbolic-metamaterial (blue), and elliptical-metamaterial (orange) structures, as a function of (a) frequency and (b) material-loss rate, for a fixed separation  $d = 0.1c/\omega_p$ . Assuming smooth surfaces, the structural parameters are computationally optimized [51] using a derivative-free local optimization algorithm [66,67]. Figure 3(b) shows that the suboptimal performance can be attributed primarily to the fact that the structures do not exhibit the material enhancement factor  $|\chi|^4 / (\text{Im}\chi)^2 \sim 1/\gamma^2$ , as predicted by Eq. (10) and due to the significant reflections in such geometries.

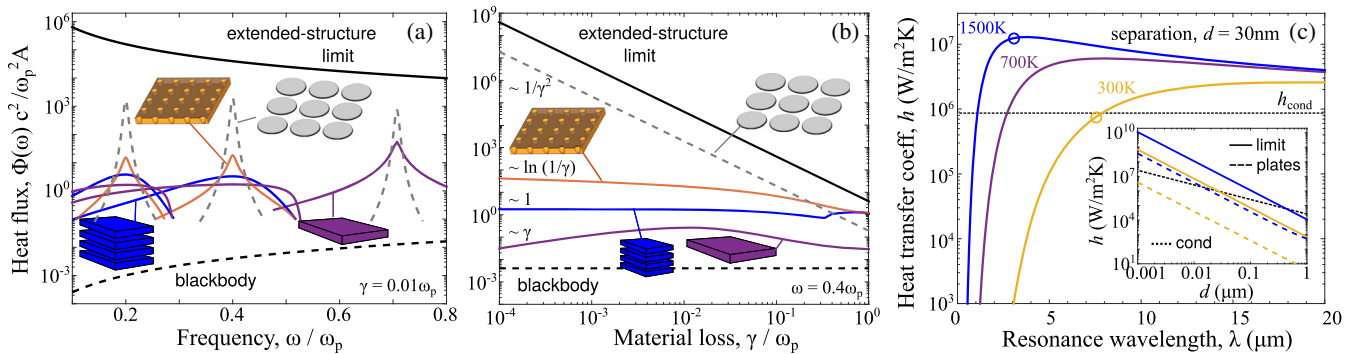


FIG. 3 (color online). (a),(b) Comparison of heat flux between mirror images of large-area Drude-metal structures separated by  $d = 0.1c/\omega_p$ . (a) Structures optimized for maximum flux at three frequencies,  $\omega = (0.2, 0.4, 1/\sqrt{2})\omega_p$ , for a material loss rate  $\gamma = 0.01\omega_p$ . Thin films (purple), hyperbolic metamaterials (blue), and elliptical metamaterials (orange) exceed blackbody enhancements but fall far short of the limit (black solid line) from Eq. (5). The dashed silver line represents the heat transfer for an idealized plasmonic-particle array without multiple scattering. (b) Optimized structures as a function of loss rate, for  $\omega = 0.4\omega_p$ . Each structure exhibits the  $1/d^2$  near-field enhancement factor, but only the idealized particle array exhibits the  $|\chi|^4 / (\text{Im}\chi)^2 \sim 1/\gamma^2$  material enhancement factor. (c) Frequency-integrated heat transfer coefficient of a structure that reaches the single-frequency limit in Eq. (5) over a narrow bandwidth  $\Delta\omega \propto \gamma$ . Radiative heat exchange in this limit shows the possibility of surpassing conductive heat transfer through air (dotted line) at  $T = 300\text{K}$  (gold line), which is not possible for plate-plate configurations (inset, dashed lines), and of significant further enhancements at higher temperatures (blue, purple lines).

The spectral heat flux of the limit in Eq. (4) can be interpreted as the exchange of enhanced free-space dipole fields, as discussed above. Guided by this intuition, we include in Figs. 3(a) and 3(b) the heat flux between close-packed arrays of oblate disk ellipsoids (dashed silver lines), small enough to be dipolar. We idealize their response as the additive sum of Eq. (8) over a lattice neglecting multiple scattering (i.e., in a Born approximation) [68] and accounting for the polarization dependence of nonspherical ellipsoids [37]. This structure combines the individual-particle interactions that exhibit the material enhancement (which planar bodies do not) with the large-area interactions that exhibit  $1/d^2$  near-field enhancement (which isolated bodies do not). Figures 3(a) and 3(b) suggest the possibility for 2 to 3 orders of magnitude enhancement by periodic structuring and tailored local interactions.

Experimental measurements of radiative heat transfer are done in vacuum [6,12,13] because radiative transfer is dominated by conductive transfer through an air gap. Achieving the limits presented here, even over a narrow bandwidth, could transform this landscape. Figure 3(c) shows the heat-transfer coefficient  $h = \int \Phi(\partial\Theta/\partial T)d\omega$  for extended Drude-metal structure with loss rates  $\gamma = 0.01\omega_p$  (appropriate, e.g., for Ag and Au [69]). For Lorentzian-shaped energy transfer with tunable center frequency  $\omega_{\text{res}} = \omega_p/\sqrt{2}$ , peaked at the limit given by Eq. (5), with a bandwidth  $\Delta\omega = \gamma$  [51,55,56], radiative transfer can surpass conductive (thermal conductivity  $\kappa_{\text{air}} = 0.026 \text{ W/m} \cdot \text{K}$  [70]) even at  $T = 300 \text{ K}$ . In the inset we fix the wavelengths at  $\lambda = 7.6 \mu\text{m}$  for  $T = 300 \text{ K}$  and  $\lambda = 3 \mu\text{m}$  for  $T = 1500 \text{ K}$ , and plot  $h$  as a function of distance for plate-plate (dashed) and optimal (solid) transfer. We find that radiative transfer can surpass conductive at separation of  $d = 50 \text{ nm}$  at  $300 \text{ K}$  and almost  $d = 0.5 \mu\text{m}$  at  $T = 1500 \text{ K}$ , gap sizes that are readily achievable in experiments.

Radiative heat transfer at the nanoscale is a nascent but growing field. Calculations have primarily been for dipolar [5,10,61] or highly symmetric bodies [8–14,18–23,25–31,71–73], with computational study of more complex geometries possible only recently [35,64,65,74–76]. Guided by the physical principles presented here, a targeted search through the mostly uncharted near-field design space offers the prospect of orders-of-magnitude enhancements in radiative energy transfer.

We thank Athanasios Polimeridis for helpful discussions. O. D. M. and S. G. J. were supported by the Army Research Office through the Institute for Soldier Nanotechnologies under Contract No. W911NF-07-D0004, and by the AFOSR Multidisciplinary Research Program of the University Research Initiative (MURI) for Complex and Robust On-chip Nanophotonics under Grant No. FA9550-09-1-0704. A. W. R. was supported by the National Science Foundation under Grant No. DMR-1454836.

- [1] D. Polder and M. Van Hove, Theory of radiative heat transfer between closely spaced bodies, *Phys. Rev. B* **4**, 3303 (1971).
- [2] S. M. Rytov, Y. A. Kravtsov, and V. I. Tatarskii, *Principles of Statistical Radiophysics* (Springer-Verlag, New York, 1988).
- [3] J.-P. Mulet, K. Joulain, R. Carminati, and J.-J. Greffet, Enhanced radiative heat transfer at nanometric distances, *Microscale Thermophys. Eng.* **6**, 209 (2002).
- [4] K. Joulain, J.-P. Mulet, F. Marquier, R. Carminati, and J.-J. Greffet, Surface electromagnetic waves thermally excited: Radiative heat transfer, coherence properties and Casimir forces revisited in the near field, *Surf. Sci. Rep.* **57**, 59 (2005).
- [5] A. I. Volokitin and B. N. J. Persson, Near-field radiative heat transfer and noncontact friction, *Rev. Mod. Phys.* **79**, 1291 (2007).
- [6] E. Rousseau, A. Siria, G. Jourdan, S. Volz, F. Comin, J. Chevrier, and J.-J. Greffet, Radiative heat transfer at the nanoscale, *Nat. Photonics* **3**, 514 (2009).
- [7] S. Basu, Z. M. Zhang, and C. J. Fu, Review of near-field thermal radiation and its application to energy conversion, *Int. J. Energy Res.* **33**, 1203 (2009).
- [8] J. J. Loomis and H. J. Maris, Theory of heat transfer by evanescent electromagnetic waves, *Phys. Rev. B* **50**, 18517 (1994).
- [9] J. B. Xu, K. Lauger, R. Moller, K. Dransfeld, and I. H. Wilson, Heat transfer between two metallic surfaces at small distances, *J. Appl. Phys.* **76**, 7209 (1994).
- [10] J. B. Pendry, Radiative exchange of heat between nanostructures, *J. Phys. Condens. Matter* **11**, 6621 (1999).
- [11] C. Fu and Z. Zhang, Nanoscale radiation heat transfer for silicon at different doping levels, *Int. J. Heat Mass Transfer* **49**, 1703 (2006).
- [12] L. Hu, A. Narayanaswamy, X. Chen, and G. Chen, Near-field thermal radiation between two closely spaced glass plates exceeding Planck's blackbody radiation law, *Appl. Phys. Lett.* **92**, 133106 (2008).
- [13] R. S. Ottens, V. Quetschke, S. Wise, A. A. Alemi, R. Lundock, G. Mueller, D. H. Reitze, D. B. Tanner, and B. F. Whiting, Near-Field Radiative Heat Transfer Between Macroscopic Planar Surfaces, *Phys. Rev. Lett.* **107**, 014301 (2011).
- [14] P. J. van Zwol, K. Joulain, P. Ben-Abdallah, and J. Chevrier, Phonon polaritons enhance near-field thermal transfer across the phase transition of VO<sub>2</sub>, *Phys. Rev. B* **84**, 161413 (2011).
- [15] S. Basu and Z. M. Zhang, Maximum energy transfer in nearfield thermal radiation at nanometer distances, *J. Appl. Phys.* **105**, 093535 (2009).
- [16] P. Ben-Abdallah and K. Joulain, Fundamental limits for noncontact transfers between two bodies, *Phys. Rev. B* **82**, 121419 (2010).
- [17] E. Nefzaoui, Y. Ezzahri, J. Drevillon, and K. Joulain, Maximal near-field radiative heat transfer between two plates, *Eur. Phys. J. Appl. Phys.* **63**, 30902 (2013).
- [18] S.-A. Biehs, P. Ben-Abdallah, F. S. S. Rosa, K. Joulain, and J.-J. Greffet, Nanoscale heat flux between nanoporous materials, *Opt. Express* **19**, A1088 (2011).

- [19] M. Francoeur, S. Basu, and S. J. Petersen, Electric and magnetic surface polariton mediated nearfield radiative heat transfer between metamaterials made of silicon carbide particles, *Opt. Express* **19**, 18774 (2011).
- [20] K. Joulain, J. Drevillon, and P. Ben-Abdallah, Noncontact heat transfer between two metamaterials, *Phys. Rev. B* **81**, 165119 (2010).
- [21] S.-A. Biehs, M. Tschikin, and P. Ben-Abdallah, Hyperbolic Metamaterials as an Analog of a Blackbody in the Near Field, *Phys. Rev. Lett.* **109**, 104301 (2012).
- [22] S.-A. Biehs, M. Tschikin, R. Messina, and P. Ben-Abdallah, Super-Planckian near-field thermal emission with phonon-polaritonic hyperbolic metamaterials, *Appl. Phys. Lett.* **102**, 131106 (2013).
- [23] Y. Guo and Z. Jacob, Thermal hyperbolic metamaterials, *Opt. Express* **21**, 15014 (2013).
- [24] E. E. Narimanov and I. I. Smolyaninov, Beyond Stefan-Boltzmann Law: Thermal Hyper-Conductivity, in *Quantum Electronics and Laser Science Conference* (Opt. Soc. Am., Washington, DC, 2012).
- [25] S.-A. Biehs, D. Reddig, and M. Holthaus, Thermal radiation and near-field energy density of thin metallic films, *Eur. Phys. J. B* **55**, 237 (2007).
- [26] M. Francoeur, M. P. Menguc, and R. Vaillon, Near-field radiative heat transfer enhancement via surface phonon polaritons coupling in thin films, *Appl. Phys. Lett.* **93**, 043109 (2008).
- [27] M. Francoeur, M. Pinar Mengüç, and R. Vaillon, Solution of near-field thermal radiation in one-dimensional layered media using dyadic Green's functions and the scattering matrix method, *J. Quant. Spectrosc. Radiat. Transfer* **110**, 2002 (2009).
- [28] P. Ben-Abdallah, K. Joulain, J. Drevillon, and G. Domingues, Near-field heat transfer mediated by surface wave hybridization between two films, *J. Appl. Phys.* **106**, 044306 (2009).
- [29] M. Francoeur, M. P. Mengüç, and R. Vaillon, Spectral tuning of near-field radiative heat flux between two thin silicon carbide films, *J. Phys. D* **43**, 075501 (2010).
- [30] S. Basu and M. Francoeur, Maximum nearfield radiative heat transfer between thin films, *Appl. Phys. Lett.* **98**, 243120 (2011).
- [31] O. D. Miller, S. G. Johnson, and A. W. Rodriguez, Effectiveness of Thin Films in Lieu of Hyperbolic Metamaterials in the Near Field, *Phys. Rev. Lett.* **112**, 157402 (2014).
- [32] M. D. Whale and E. G. Cravalho, Modeling and performance of microscale thermophotovoltaic energy conversion devices, *IEEE Trans. Energy Convers.* **17**, 130 (2002).
- [33] M. Laroche, R. Carminati, and J.-J. Greffet, Near-field thermophotovoltaic energy conversion, *J. Appl. Phys.* **100**, 063704 (2006).
- [34] P. Bermel, M. Ghebrebrhan, W. Chan, Y. X. Yeng, M. Araghchini, R. Hamam, C. H. Marton, K. F. Jensen, M. Soljačić, J. D. Joannopoulos, S. G. Johnson, and I. Celanovic, Design and global optimization of high-efficiency thermophotovoltaic systems, *Opt. Express* **18**, A314 (2010).
- [35] A. W. Rodriguez, O. Ilic, P. Bermel, I. Celanovic, J. D. Joannopoulos, M. Soljačić, and S. G. Johnson, Frequency-Selective Near-Field Radiative Heat Transfer between Photonic Crystal Slabs: A Computational Approach for Arbitrary Geometries and Materials, *Phys. Rev. Lett.* **107**, 114302 (2011).
- [36] J. H. Lienhard IV and J. H. Lienhard V, *A Heat Transfer Textbook*, 4th ed. (Dover, New York, 2011).
- [37] C. F. Bohren and D. R. Huffman, *Absorption and Scattering of Light by Small Particles* (John Wiley & Sons, New York, NY, 1983).
- [38] S. G. Johnson, P. Bienstman, M. A. Skorobogatiy, M. Ibanescu, E. Lidorikis, and J. D. Joannopoulos, Adiabatic theorem and continuous coupled-mode theory for efficient taper transitions in photonic crystals, *Phys. Rev. E* **66**, 066608 (2002).
- [39] D.-H. Kwon and D. M. Pozar, Optimal Characteristics of an Arbitrary Receive Antenna, *IEEE Trans. Antennas Propag.* **57**, 3720 (2009).
- [40] I. Liberal, Y. Ra'di, R. Gonzalo, I. Eterra, S. A. Tretyakov, and R. W. Ziolkowski, Least Upper Bounds of the Powers Extracted and Scattered by Bianisotropic Particles, *IEEE Trans. Antennas Propag.* **62**, 4726 (2014).
- [41] J.-P. Hugonin, M. Besbes, and P. Ben-Abdallah, Fundamental limits for light absorption and scattering induced by cooperative electromagnetic interactions, *Phys. Rev. B* **91**, 180202 (2015).
- [42] O. D. Miller, A. G. Polimeridis, M. T. H. Reid, C. W. Hsu, B. G. DeLacy, J. D. Joannopoulos, M. Soljačić, and S. G. Johnson, Fundamental limits to the optical response of lossy media, [arXiv:1503.03781](https://arxiv.org/abs/1503.03781).
- [43] D. A. B. Miller, Communicating with waves between volumes: evaluating orthogonal spatial channels and limits on coupling strengths, *Appl. Opt.* **39**, 1681 (2000).
- [44] J. D. Jackson, *Classical Electrodynamics*, 3rd ed. (John Wiley & Sons, New York, 1999).
- [45] R. G. Newton, Optical theorem and beyond, *Am. J. Phys.* **44**, 639 (1976).
- [46] D. R. Lytle, P. S. Carney, J. C. Schotland, and E. Wolf, Generalized optical theorem for reflection, transmission, and extinction of power for electromagnetic fields, *Phys. Rev. E* **71**, 056610 (2005).
- [47] H. Hashemi, C.-W. Qiu, A. P. McCauley, J. D. Joannopoulos, and S. G. Johnson, Diameter-bandwidth product limitation of isolated-object cloaking, *Phys. Rev. A* **86**, 013804 (2012).
- [48] W. C. Chew, *Waves and Fields in Inhomogeneous Media* (IEEE Press, New York, 1995), Vol. 522.
- [49] L. N. Trefethen and D. Bau, *Numerical Linear Algebra* (Society for Industrial and Applied Mathematics, Philadelphia, PA, 1997).
- [50] E. J. Rothwell and M. J. Cloud, *Electromagnetics* (CRC Press, Boca Raton, 2001).
- [51] See Supplemental Material at <http://link.aps.org/supplemental/10.1103/PhysRevLett.115.204302> for heat-transfer approximations for a variety of structures and asymptotic limits, which includes Refs. [52] and [53].
- [52] M. Cardona, Fresnel Reflection and Surface Plasmons, *Am. J. Phys.* **39**, 1277 (1971).
- [53] J. A. Kong, *Theory of Electromagnetic Waves* (Wiley-Interscience, New York, 1975), Vol. 1.
- [54] R. Piestun and D. A. B. Miller, Electromagnetic degrees of freedom of an optical system, *J. Opt. Soc. Am. A* **17**, 892 (2000).

- [55] F. Wang and Y.R. Shen, General Properties of Local Plasmons in Metal Nanostructures, *Phys. Rev. Lett.* **97**, 206806 (2006).
- [56] A. Raman, W. Shin, and S. Fan, Upper Bound on the Modal Material Loss Rate in Plasmonic and Metamaterial Systems, *Phys. Rev. Lett.* **110**, 183901 (2013).
- [57] F. Singer, Y. Ezzahri, and K. Joulain, Near field radiative heat transfer between two nonlocal dielectrics, *J. Quant. Spectrosc. Radiat. Transfer* **154**, 55 (2015).
- [58] O. D. Miller *et al.* (to be published).
- [59] C. Ciraci, R. T. Hill, J. J. Mock, Y. Urzhumov, A. I. Fernández-Domínguez, S. A. Maier, J. B. Pendry, A. Chilkoti, and D. R. Smith, Probing the Ultimate Limits of Plasmonic Enhancement, *Science* **337**, 1072 (2012).
- [60] S. Raza, S. I. Bozhevolnyi, M. Wubs, and N. Asger Mortensen, Nonlocal optical response in metallic nanostructures, *J. Phys. Condens. Matter* **27**, 183204 (2015).
- [61] J. P. Mulet, K. Joulain, R. Carminati, and J. J. Greffet, Nanoscale radiative heat transfer between a small particle and a plane surface, *Appl. Phys. Lett.* **78**, 2931 (2001).
- [62] S. A. Maier, *Plasmonics: Fundamentals and Applications* (Springer Science & Business Media, New York, 2007).
- [63] M. T. H. Reid, <http://homerreid.com/scuff-EM>.
- [64] A. W. Rodriguez, M. T. Homer Reid, and S. G. Johnson, Fluctuating-surface-current formulation of radiative heat transfer for arbitrary geometries, *Phys. Rev. B* **86**, 220302 (2012).
- [65] A. W. Rodriguez, M. T. H. Reid, and S. G. Johnson, Fluctuating-surface-current formulation of radiative heat transfer: Theory and applications, *Phys. Rev. B* **88**, 054305 (2013).
- [66] M. J. D. Powell, in *Advances in Optimization and Numerical Analysis* (Springer, New York, 1994), p. 51.
- [67] S. G. Johnson, <http://ab-initio.mit.edu/nlopt>.
- [68] A. D. Phan, T.-L. Phan, and L. M. Woods, Near-field heat transfer between gold nanoparticle arrays, *J. Appl. Phys.* **114**, 214306 (2013).
- [69] E. D. Palik, *Handbook of Optical Constants of Solids*, edited by E. D. Palik (Elsevier Science, New York, 1998).
- [70] W. M. Haynes, *CRC Handbook of Chemistry and Physics* (CRC Press, Boca Raton, 2013).
- [71] C. Otey and S. Fan, Numerically exact calculation of electromagnetic heat transfer between a dielectric sphere and plate, *Phys. Rev. B* **84**, 245431 (2011).
- [72] A. Perez-Madrid, L. C. Lapas, and J. M. Rubi, A thermokinetic approach to radiative heat transfer at the nanoscale, *PLoS One* **8**, e58770 (2013).
- [73] Y. Zheng and A. Ghanekar, Radiative energy and momentum transfer for various spherical shapes: A single sphere, a bubble, a spherical shell, and a coated sphere, *J. Appl. Phys.* **117**, 064314 (2015).
- [74] A. P. McCauley, M. T. H. Reid, M. Krüger, and S. G. Johnson, Modeling near-field radiative heat transfer from sharp objects using a general three-dimensional numerical scattering technique, *Phys. Rev. B* **85**, 165104 (2012).
- [75] A. Pérez-Madrid, J. M. Rubí, and L. C. Lapas, Heat transfer between nanoparticles: Thermal conductance for near-field interactions, *Phys. Rev. B* **77**, 155417 (2008).
- [76] C. R. Otey, L. Zhu, S. Sandhu, and S. Fan, Fluctuational electrodynamics calculations of near-field heat transfer in non-planar geometries: A brief overview, *J. Quant. Spectrosc. Radiat. Transfer* **132**, 3 (2014).